Available online at www.sciencedirect.com

ScienceDirect

IFAC Papers Online CONFERENCE PAPER ARCHIVE

IFAC-PapersOnLine 49-18 (2016) 606–611

Attitude & Position Tracking of a Underwater Rigid Body

Arun Kumar S * **Rakesh R. Warier** * **Srikant Sukumar** *

* *Indian Institute of Technology, Bombay, India (e-mail: {arunkumar92,rakeshwarier,srikant}@sc.iitb.ac.in).*

Abstract: This paper deals with attitude and position tracking of rigid bodies immersed in a fluid (generally water) and proposes a control law to achieve the same. Underwater dynamics of rigid bodies are modelled using the 'Kirchhoff Tensor', assuming the fluid to be irrotational, inviscid and incompressible. Specifically we consider the case of asymmetrical rigid bodies, where the dynamics of the rotational and translational motions are coupled with each other. The proposed control law is proven to asymptotically converge to the desired trajectory by analytical methods as well as in simulations.

Keywords: Underwater Rigid-Body Tracking Attitude

1. INTRODUCTION

Unmanned underwater vehicles can be employed for variety of applications like exploration, mapping, search and rescue. The wide range of applications of AUVs (Autonomous Underwater Vehicles) has been explored by Bogue et al. (2015). The use of AUVs for seabed health monitoring, inspecting oil spills and prediction of natural calamities like tsunamis or hurricanes has been surveyed by Campbell et al. (2015) and Felemban et al. (2015). Design of control laws for these vehicles require modeling their underwater motion. Underwater dynamics are difficult to calculate in real-time owing to their computational intensity. Control design of vehicles underwater is also challenging because the viscosity and density of water is significantly higher than that of air which gives rise to many phenomena that are specific to underwater vehicles.

One significant phenomenon is the interdependence of translational and rotational motions of asymmetric bodies immersed in water. This means that a force along an axis of the body can cause a rotation and similarly a torque along an axis can cause the body to translate. So the control design for the rotational and translational motion cannot be done independently. Kirchhoff (1869) proposed a model in which this phenomenon is accounted for by just modifying the moment of inertia tensor (into what is called the *kirchhoff tensor*) in the rigid body equations in free space. This is only a pre-computation step and does not require modeling the flow of fluid particles in real-time. The numerical method to calculate the *kirchhoff tensor* is explained in detail in Weißmann and Pinkall (2012). The equations of motions with the *kirchhoff tensor*, known as the *kirchhoff* equations have been studied in Holmes et al. (1998) and Leonard (1997). Design of control laws for multiple rigid bodies with dynamics defined by *kirchhoff* equations has been done in Nair and Leonard (2007). However, in the aforementioned literature, only symmetric bodies are considered where the linear and angular momenta of the body are decoupled. In this paper, we relax the assumption that the body is symmetric and work with a general dynamic model which will work for asymmetric bodies as well.

Attitude tracking of a rigid body in space without the knowledge of inertia tensor has been done by Sanyal et al. (2009). Combined position and attitude tracking was done by Lee et al. (2010). In this paper we consider the attitude and position tracking problem of a underwater rigid body to a trajectory whose parameters are supplied in real time. Here, the primary difference is the coupling of attitude and translational dynamics due to the *kirchhoff* tensor. We achieve an almost global region of convergence (as defined in Bayadi and Banavar (2014)) with the proposed control law.

Section 2.1 has a few mathematical preliminaries that are used in the proof and section 2.2 gives an overview of the *kirchhoff* tensor. The problem is formulated and error functions are defined in section 3. The proposed control law is stated and asymptotic stability is proved in section 4. Simulation results are displayed in section 5 and the conclusions are discussed in section 6.

2. PRELIMINARIES

2.1 Mathematical Preliminaries

In this section we list the properties of a few functions and notions beforehand for referencing in the proofs. Also some conventions followed are mentioned.

Rotation Matrix : A rotation matrix usually denoted by $R \in SO(3) = \{\mathbb{R}^{3\times3} | RR^T = I_3,\ |R| = 1\}$($I_3$ is the identity matrix of order 3) represents the attitude of a rigid body with respect to a fixed inertial frame. It maps vectors from inertial coordinates to corresponding coordinates in body-centric frame and vice-versa. In this paper we follow the convention that the rotation matrix R of a rigid body

2405-8963
Peer review under responsibility of International Federation of Automatic Control.
10.1016/j.ifacol.2016.10.232

takes a vector from body-centric frame($\mathbb{R}^3$) to the inertial frame($\mathbb{R}^3$), while R^T does the inverse.

Hat and Inverse hat maps : The hat map($\wedge$) is an isomorphism from $\mathbb{R}^3$ to $so(3) = \{S \in \mathbb{R}^{3\times3} | S^T = -S\}$. For a given vector $\omega = [\omega_1\ \omega_2\ \omega_3]^T$,

$$\widehat{\omega} = \begin{bmatrix} 0 & -\omega_3 & \omega_2 \\ \omega_3 & 0 & -\omega_1 \\ -\omega_2 & \omega_1 & 0 \end{bmatrix}$$

The inverse hat map($\vee$) maps real skew-symmetric matrices of order 3 ($so(3)$) to the corresponding vectors in $\mathbb{R}^3$.

One particular property of hat operator that will be frequently used (Sanyal et al. (2009)) is

$$R\widehat{\omega}R^T = (R\omega)^\wedge \tag{1}$$

where R is a rotation matrix .

Trace Function : Trace of a square matrix M denoted by $tr(M)$ is the sum of the diagonal elements. We define two functions skew() and sym() which break down a given square matrix into symmetric and skew symmetric components. For a square matrix M, $\text{skew}(M) = \frac{M-M^T}{2}$ and $\text{sym}(M) = \frac{M+M^T}{2}$. So for a given matrix M of order 3 and a vector ω of order 3,

$$tr(\text{sym}(M)\widehat{\omega}) = 0 \tag{2}$$

$$tr(\text{skew}(M)\widehat{\omega}) = -2((skew(M))^\wedge)^T\omega \tag{3}$$

These identities can easily be verified algebraically.

The derivative of a function $f(t)$ with respect to time has been represented by the notations $\frac{df}{dt}$ and $\dot{f}$ interchangeably.

2.2 Kirchhoff Tensor

The *kirchhoff* tensor is a modification of the inertia tensor of a rigid body in free space. For a body in space with linear and angular velocities $\omega \in \mathbb{R}^3$ and $v \in \mathbb{R}^3$, the respective momenta $l \in \mathbb{R}^3$ and $p \in \mathbb{R}^3$ are

$$\begin{bmatrix} l \\ p \end{bmatrix} = \begin{bmatrix} J_B & 0 \\ 0 & mI_3 \end{bmatrix} \begin{bmatrix} \omega \\ v \end{bmatrix} \tag{4}$$

Where $J_B \in \mathbb{R}^{3\times3}$ is the moment of inertia matrix, $m \in \mathbb{R}$ is the mass of body. In the case of underwater bodies the modified equation becomes,

$$\begin{bmatrix} l \\ p \end{bmatrix} = K \begin{bmatrix} \omega \\ v \end{bmatrix} \tag{5}$$

Where $K \in \mathbb{R}^{6\times6}$ is the *kirchhoff* tensor which is a function of the density of the fluid under consideration and the geometry of the immersed rigid body. K can be partitioned into 3×3 matrices as

$$K = \begin{bmatrix} J & P^\top \\ P & M \end{bmatrix}. \tag{6}$$

It can be seen that while J and M are similar to the case of rigid body in air, the matrix P represents the coupling between angular and linear momenta. A detailed explanation of the *kirchhoff* tensor and a numerical method to compute the same can be found in Weißmann and Pinkall (2012). For asymmetric rigid bodies, the matrix P is non-zero which ensures coupling between translational and rotational momenta. In this paper we shall only consider the cases where P is non-zero. It is also important to note that this formulation has been derived under the assumptions that the fluid is irrotaional, inviscid, incompressible and its flow is a potential flow. These assumptions serve to reduce the computational complexity and thus enable real-time implementation.

3. PROBLEM FORMULATION

3.1 Equation of Dynamics

The equation of dynamics of underwater rigid body as described in Section 2.2 are

$$\dot{R} = R\widehat{\omega} \tag{7}$$

$$\dot{x} = Rv \tag{8}$$

$$\begin{bmatrix} l \\ p \end{bmatrix} = K \begin{bmatrix} \omega \\ v \end{bmatrix} = \begin{bmatrix} J\omega + P^T v \\ P\omega + Mv \end{bmatrix} \tag{9}$$

$$\begin{bmatrix} \dot{l} \\ \dot{p} \end{bmatrix} = \begin{bmatrix} J\dot{\omega} + P^T\dot{v} \\ P\dot{\omega} + M\dot{v} \end{bmatrix} = \begin{bmatrix} l \times \omega + p \times v \\ p \times \omega \end{bmatrix} + \begin{bmatrix} \tau \\ f \end{bmatrix} \tag{10}$$

Where $\tau \in \mathbb{R}^3$ and $f \in \mathbb{R}^3$ are the control torque and force applied respectively in the body fixed frame. $l, p \in \mathbb{R}^3$ are the linear and angular momentum of the rigid body in fluid represented in the body fixed frame. v, $\omega \in \mathbb{R}^3$ are the linear and angular velocities of the body respectively, measured in the body fixed frame. R is the rotation matrix that represents the attitude of the body frame with respect to the inertial frame. $x \in \mathbb{R}^3$ is the position of the origin of the body centric frame with respect to the inertial frame.

We want the rigid body vehicle underwater to follow a desired smooth varying trajectory given by $R_d(t)$, $\omega_d(t)$, $x_d(t)$ and $v_d(t)$) satisfying following kinematic conditions

$$\dot{R}_d = R_d\widehat{\omega}_d \tag{11}$$

$$\dot{x}_d = R_d v_d \tag{12}$$

3.2 Error Variables

Given the system states R, ω, x, v and the corresponding desired system variables R_d, x_d (in inertial frame), ω_d, v_d we define the following error variables - attitude error R_e, position error x_e, angular velocity error ω_e and linear velocity error v_e - to be,

$$R_e = R_d^T R \tag{13}$$

$$x_e = x - x_d \tag{14}$$

$$\omega_e = \omega - R_e^T\omega_d \tag{15}$$

$$v_e = v - R_e^T v_d. \tag{16}$$

Their derivatives are,

$$\dot{R}_e = R_e\widehat{\omega}_e \tag{17}$$
$$\dot{x}_e = R(v - R_e^T v_d) \tag{18}$$
$$\dot{\omega}_e = \dot{\omega} - \dot{R}_e^T\omega_d - R_e^T\dot{\omega}_d \tag{19}$$
$$\dot{v}_e = \dot{v} - \dot{R}_e^T v_d - R_e^T\dot{v}_d. \tag{20}$$

3.3 Error Functions

Velocity error functions and position error function are taken to be quadratic functions of their corresponding error variables. Attitude error function is usually expressed by a modified trace function as done in Warier et al. (2014), Chaturvedi et al. (2011) and Sarlette et al. (2009). We define the attitude error function $\Delta(R_e)$ for rotation matrix R_e as

$$\Delta_1(R_e) = tr\left(A - AR_e\right) \tag{21}$$

here A is chosen to be $A = \text{diag}([a_1,\ a_2,\ a_3])$, with $a_3 > a_2 + a_1 > 0$. It can be seen that this function attains a minimum of 0 when $R_d^T R = I_3 \Rightarrow R_e = I_3$.

3.4 Control Objectives

The control objective can be mathematically defined as

(1)	$R \longrightarrow R_d$	$\Rightarrow$	$R_e \longrightarrow I_3$
(2)	$x \longrightarrow x_d$	$\Rightarrow$	$x_e \longrightarrow 0$
(3)	$\omega \longrightarrow R_e^T\omega_d$	$\Rightarrow$	$\omega_e \longrightarrow 0$
(4)	$v \longrightarrow R_e^T v_d$	$\Rightarrow$	$v_e \longrightarrow 0$

4. CONTROL LAW

We propose the following control law,

$$\begin{aligned}\tau = &-\left(J\omega\times\omega + P^T v\times\omega + P\omega\times v + Mv\times v + \right.\\ &J\widehat{\omega}_e R_e^T\omega_d - JR_e^T\dot{\omega}_d + P^T\widehat{\omega}_e R_e^T v_d\\ &\left. - P^T R_e^T\dot{v}_d\right) - \gamma_1\,\text{skew}(AR_e)^\vee - \alpha\omega_e \end{aligned}\tag{22}$$

$$\begin{aligned}f = &-\left(P\omega\times\omega + Mv\times\omega + P\widehat{\omega}_e R_e^T\omega_d - PR_e^T\dot{\omega_d} + \right.\\ &\left. M\widehat{\omega}_e R_e^T v_d - MR_e^T\dot{v_d}\right) - \gamma_2 R^T(x_e) - \beta v_e \end{aligned}\tag{23}$$

Where α, β,γ_1, $\gamma_2 > 0$.

We lay forward the following proposition.

Proposition 1. Consider transformed system with states $(R_e, \omega_e, x_e, v_e)$ defined in (13) - (16) with the system dynamics defined by equations (7), (8), (9) and (10), under the control law defined by equations (22)-(23). We have the following :

(i) The positive limit set of the closed loop system are given by $\mathcal{L} = \{(R_e, \omega_e, x_e, v_e)|\, R_e \in N,\ x_e = 0,\ \omega_e = 0,\ v_e = 0\}$, where N is given by
$$N = \{I_3, \text{diag}(1,-1,-1), \text{diag}(-1,-1,1), \text{diag}(1,1,-1)\}.$$
(ii) The desired equilibrium configuration $\mathcal{L}_1$, given by $\mathcal{L}_1 = \Big(I_3, 0, 0, 0\Big)$, $\mathcal{L}_1 \subset \mathcal{L}$, is almost globally stable.

Proof.

(i) Consider $\mathcal{V}$ as the candidate lyapunov function defined as

$$\mathcal{V} = \frac{1}{2}\gamma_1\Delta_1 + \frac{1}{2}\gamma_2\Delta_2 + \frac{1}{2}\Delta_3 \tag{24}$$

Where,

$$\Delta_1(R_e) = tr\left(A - AR_e\right) \tag{25}$$
$$\Delta_2(x_e) = x_e^T x_e \tag{26}$$
$$\Delta_3(\omega_e, v_e) = \begin{bmatrix}\omega_e\\ v_e\end{bmatrix}^T K \begin{bmatrix}\omega_e\\ v_e\end{bmatrix} \tag{27}$$
$$\tag{28}$$

$\dot{\mathcal{V}}$ will then be

$$\dot{\mathcal{V}} = \frac{1}{2}\gamma_1\dot{\Delta}_1 + \frac{1}{2}\gamma_2\dot{\Delta}_2 + \frac{1}{2}\dot{\Delta}_3 \tag{29}$$

Where,

$$\begin{aligned}\dot{\Delta}_3 =& 2\begin{bmatrix}\omega_e\\ v_e\end{bmatrix}.\left(K\begin{bmatrix}\dot{\omega_e}\\ \dot{v_e}\end{bmatrix}\right)\\ =& 2\begin{bmatrix}\omega_e\\ v_e\end{bmatrix}.\left(K\begin{bmatrix}\dot{\omega} - \frac{d}{dt}\left(R_e^T\omega_d\right)\\ \dot{v} - \frac{d}{dt}\left(R_e^T v_d\right)\end{bmatrix}\right)\\ =& 2\begin{bmatrix}\omega_e\\ v_e\end{bmatrix}.\begin{bmatrix}\dot{l} - J\frac{d}{dt}\left(R_e^T\omega_d\right) - P^T\frac{d}{dt}\left(R_e^T v_d\right)\\ \dot{p} - P\frac{d}{dt}\left(R_e^T\omega_d\right) - M\frac{d}{dt}\left(R_e^T v_d\right)\end{bmatrix}\end{aligned}\tag{30}$$

Substituting equations (10) , we get

$$\begin{aligned}\dot{\Delta}_3 =& 2\omega_e.(J\omega\times\omega + P^T v\times\omega + P\omega\times v + Mv\times v +\\ & J\widehat{\omega}_e R_e^T\omega_d - JR_e^T\dot{\omega}_d + P^T\widehat{\omega}_e R_e^T v_d - P^T R_e^T\dot{v}_d\\ & + \tau) + 2v_e.(P\omega\times\omega + Mv\times\omega + P\widehat{\omega}_e R_e^T\omega_d\\ & - PR_e^T\dot{\omega}_d + M\widehat{\omega}_e R_e^T v_d - MR_e^T\dot{v}_d + f)\end{aligned}\tag{31}$$

Similarly,

$$\begin{aligned}\dot{\Delta}_1 =& -tr(-A\widehat{\omega}_d R_e + AR_e\widehat{\omega})\\ =& -tr(AR_e(\widehat{\omega} - R_e^T\widehat{\omega}_d R_e))\end{aligned}\tag{32}$$

We know that $R_e^T\widehat{\omega}_d R = (R_e^T\omega_d)^\wedge$ from equation (1) . Also using the property of trace functions defined by equations (2) and (3) , we get

$$\begin{aligned}\dot{\Delta}_1 =& -tr(AR_e(\omega - R_e^T\omega_d)^\wedge)\\ =& 2\,\text{skew}(AR_e)^\vee.((\omega - R_e^T\omega_d))\\ =& 2\,\text{skew}(AR_e)^\vee.\omega_e\end{aligned}\tag{33}$$

Also,

$$\begin{aligned}\dot{\Delta}_2 =& 2.(Rv - R_d v_d).(x_e)\\ =& 2.R(v - R_e^T v_d).(x_e)\\ =& 2R^T(x_e).(v_e)\end{aligned}\tag{34}$$

Substituting equations (31),(33),(34), (22) and (23) in equation (29) we have,

$$\begin{aligned}\dot{\mathcal{V}} =& \gamma_1((\text{skew}(AR_e))^\vee.\omega_e) + \gamma_2(R^T(x_e).(v_e)) +\\ & \omega_e.(-\gamma_1(\text{skew}(AR_e))^\vee - \alpha\omega_e) +\\ & v_e.(-\gamma_2 R^T(x_e) - \beta v_e)\end{aligned}\tag{35}$$

$$= -\alpha\left\|\omega_e\right\|^2 - \beta\left\|v_e\right\|^2 \leq 0 \tag{36}$$

This proves that the system is stable. To compute the positive limit set we make use of La-Salle's invariance principle.

The closed loop dynamics of the system with the proposed control law will be,

$$\begin{aligned}\dot{l} =& J\frac{d}{dt}(R_e^T\omega_d) + P^T\frac{d}{dt}(R_e^T v_d) \\ & - \gamma_1 \operatorname{skew}(AR_e)^\vee - \alpha\omega_e \qquad (37)\\ \dot{p} =& P\frac{d}{dt}(R_e^T\omega_d) + M\frac{d}{dt}(R_e^T v_d) \\ & - \gamma_2 R^T(x_e) - \beta v_e \qquad (38)\end{aligned}$$

Consider the set $E = \{(R_e, \omega_e, x_e, v_e) | \dot{\mathcal{V}} = 0\}$. The trajectories contained in the set E would be the set of points defined by $\omega_e = v_e = 0$ i.e. $\omega = R_e^T\omega_d$ and $v = R_e^T v_d$. Substituting these constraints in equation (37) and (38), we get

$$\begin{aligned}\dot{l} =& J\frac{d}{dt}(\omega) + P^T\frac{d}{dt}(v) + \frac{\gamma_2}{\gamma_1}\operatorname{skew}(AR_e)^\vee \\ \dot{p} =& P\frac{d}{dt}(\omega) + M\frac{d}{dt}(v) - \frac{\gamma_3}{\gamma_1}R^T(x_e)\end{aligned}$$

But $\dot{l} = J\dot{\omega} + P^T\dot{v}$ and $\dot{p} = P\dot{\omega} + M\dot{v}$ from equations (10). So this implies that

$$\begin{aligned}\gamma_1 \operatorname{skew}(AR_e)^\vee &= 0 \\ \gamma_2 R^T(x_e) &= 0.\end{aligned}$$

Thus we have $x_e = 0$ and $R_e \in N$. So the set $\mathcal{L} = \{(R_e, \omega_e, x_e, v_e) |\, R_e \in N,\, x_e = 0,\, \omega_e = 0,\, v_e = 0\}$ forms the positive limit set for the closed loop system.

(ii) This is done in two steps. First we will prove that $\mathcal{L}_1$ is locally asymptotically stable and secondly we will prove $\mathcal{L}\backslash\mathcal{L}_1$ to be unstable.

From (24) we have $\mathcal{V} = 0$ only at $\mathcal{L}_1$, and $\mathcal{V} > 0$ elsewhere. Also from (36), $\dot{\mathcal{V}} \leq 0$, this gives the Lyapunov stability of $\mathcal{L}_1$.

Consider a region of attraction defined as

$$\begin{aligned}&\Delta_1(0) < a_1 + a_2 \qquad (39)\\ &\frac{1}{2}\lambda_{\max}(K)\big(\|\omega_e(0)\|^2 + \|v_e(0)\|^2\big) + \frac{1}{2}\gamma_2\Delta_2(0) \\ &\qquad < \gamma_1(a_1 + a_2) - \gamma_1\Delta_1(0) \qquad (40)\end{aligned}$$

where $\lambda_{\max}$ represents the largest eigenvalue, and a_1, a_2 are smallest eigenvalues of the gain matrix A. Conditions (39)-(40) on initial states R_e, ω_e, x_e, v_e gives,

$$\mathcal{V}(0) < \gamma_1(a_1 + a_2) \qquad (41)$$

Since $\dot{\mathcal{V}} \leq 0$,

$$0 \leq \mathcal{V}(t) < \mathcal{V}(0) < \gamma_1(a_1 + a_2) \qquad (42)$$

Thus when (39)-(40) are satisfied system dynamics converge to desired configuration $\mathcal{L}_1$. This combined with Lyapunov stability gives local asymptotic stability of $\mathcal{L}_1$.

We want to show that undesired equilibria given by $\mathcal{L}_0 = \{(R_e, \omega_e, x_e, v_e) |\, R_e \neq I, R_e \in N,\, x_e = 0,\, \omega_e = 0,\, v_e = 0\}$ are unstable. Let us consider one such configuration given as

$$\begin{aligned}G =& \{(R_e, \omega_e, x_e, v_e) |\, R_e = \operatorname{diag}([-1,\ -1,\ 1]), \\ & x_e = 0,\, \omega_e = 0,\, v_e = 0\} \qquad (43)\end{aligned}$$

From substitution we have $\mathcal{V}_G = \gamma_1(a_1 + a_2)$. We define $\mathcal{W} = \gamma_1(a_1 + a_2) - \mathcal{V}$. In sufficiently close neighbourhood to G, $\mathcal{W}$ is positive definite and $\dot{\mathcal{W}} = -\dot{\mathcal{V}} > 0$. Thus by Chetaev's theorem (Khalil (2002), Theorem 3.3) in arbitrarily small neighbourhood around configuration G, there exists a solution trajectory that will escape, and hence G is unstable. Similar arguments can be made for other configurations in $\mathcal{L}_0$.

Since any configuration $\mathcal{G} \in \mathcal{L}_0$ is unstable, from theorem 3.2.1 of Guckenheimer and Holmes (1983) each of them have non trivial unstable manifolds. Thus union of stable manifolds of three undesired equilibria are lower dimensional than the tangent space $T\mathrm{SO}(3) \times \mathbb{R}^3 \times \mathbb{R}^6$ and therefore, its measure is zero. Any solution starting from outside of this zero-measure set asymptotically converges to the desired equilibrium configuration $\mathcal{L}_1$. Thus $\mathcal{L}_1$ is almost globally asymptotically stable. Similar arguments have been used in Sanyal et al. (2009).

5. SIMULATIONS

The motion of a propeller shaped object was simulated using MATLAB$^{\mathrm{TM}}$ for the above control laws. The *kirchhoff* tensor was calculated using the algorithm mentioned in Weißmann and Pinkall (2012). The *kirchhoff* tensor so obtained, in terms of its partitioned matrices was

$$J = \begin{bmatrix} 1.359 & 0 & 0 \\ 0 & 1.8102 & -0.0002 \\ 0 & 0 & 1.3595 \end{bmatrix} Kg\,m^2$$

$$P = \begin{bmatrix} 0.50303 & 0 & 0 \\ 0 & -1.0130 & 0.0003 \\ 0 & -0.0004 & 0.5038 \end{bmatrix} Kg\,m$$

$$M = \begin{bmatrix} 0.9490 & 0 & 0 \\ 0 & 2.4167 & 0.0002 \\ 0 & 0.00117 & 0.9495 \end{bmatrix} Kg$$

The propeller was assumed to have an initial position $x(0) = [0\ 0\ 0]^T m$, initial orientation $R(0) = exp(\frac{\pi}{5}\hat{z})$ where $z = [0\ 0\ 1]^T$, initial velocity $v(0) = [1\ 2\ 0.25]^T ms^{-1}$ and initial angular velocity $\omega(0) = [0.1\ 0.1\ 0.5]^T rad\,s^{-1}$. The trajectory to be tracked was evolved by numerical integration with $\dot{\omega}_d = [0.1\,sin(t)\ 0.1\,cos(t)\ 0]^T rad\,s^{-2}$ and $\dot{v}_d = [sin(t)\ cos(t)\ 0]^T ms^{-2}$. We choose $\gamma_1 = 0.1\,, \gamma_2 = 1$ and $A = diag(10, 11, 12)$.

Figures (1) and (2) are plots of the attitude error function $\Delta_1(R_e)$ and norm of the position error function $\|x_e\|$ respectively for the cases of using the control as described by (22) - (23) and using $P = 0$ in the aforementioned control equations to show a comparison between the responses of the controller with and without modeling the coupling. Figure (3) is a plot of the norm of velocity error variables $\|\omega_e\|$ and $\|v_e\|$ with time. The corresponding control torque and force applied are plotted in figures (4) and (5) respectively.

It can be observed that when coupling is not considered ($P = 0$), the attitude and position errors do not converge to zero while all errors converge to zero when coupling

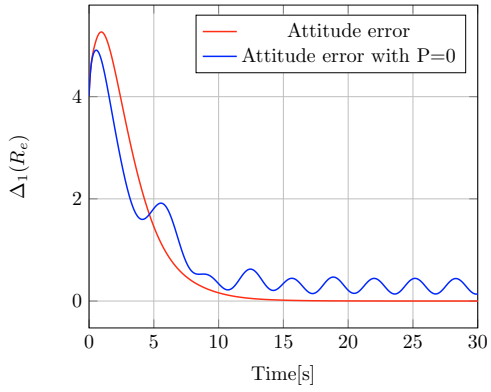

Fig. 1. Variation of attitude error $\Delta_1(R_e)$ with time for control with zero and non-zero P

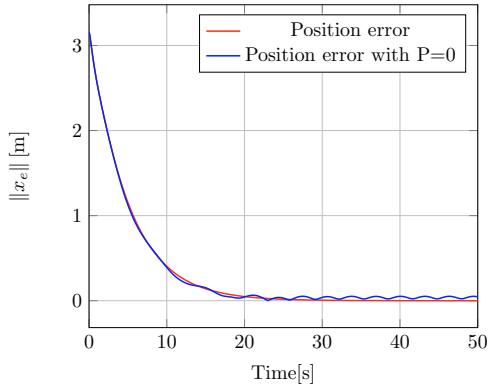

Fig. 2. Variation of position error $\|x_e\|$ with time for control with zero and non-zero P

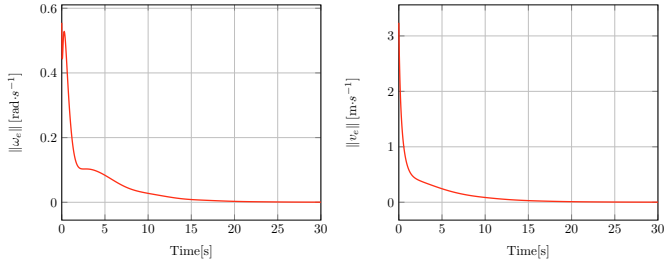

(a) Variation of angular velocity error $\|\omega_e\|$ with time

(b) Variation of velocity error $\|v_e\|$ with time

Fig. 3. Variation of velocity error functions with time

is considered. The rates of convergence can be modified by choosing γ_1 and γ_2 appropriately. Also some components of control torque and force have non-zero steady state values indicating the dynamic nature of the desired trajectory.

6. CONCLUSIONS

In this paper we proposed a control law for tracking of position and attitude of a underwater rigid body with coupled linear and angular momenta. We used the *kirchhoff* tensor to model the aforementioned coupling. Under the proposed control law, the states converge to the desired trajectory asymptotically with a almost global region of convergence.

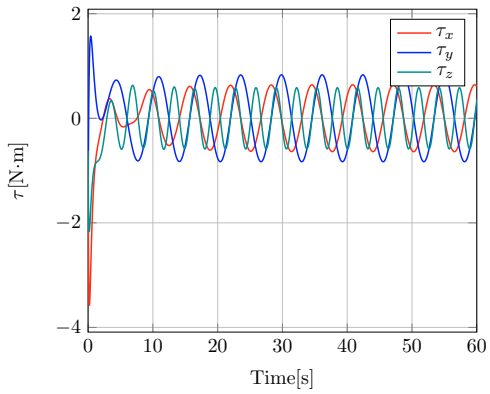

Fig. 4. Control Torque applied

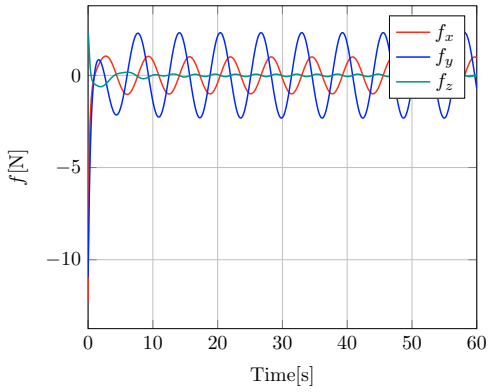

Fig. 5. Control Force applied

This work can be extended to synchronization of multiple rigid bodies along the lines of Warier et al. (2014). Another possible direction of work is using an adaptation scheme to dynamically compute the *kirchhoff* tensor so as to account for the errors arising due to assumptions on the fluid and inaccuracies in modelling of the system.

REFERENCES

Bayadi, R. and Banavar, R.N. (2014). Almost global attitude stabilization of a rigid body for both internal and external actuation schemes. *European Journal of Control*, 20(1), 45–54.

Bogue, R., Loughlin, C., and Loughlin, C. (2015). Underwater robots: a review of technologies and applications. *Industrial Robot: An International Journal*, 42(3).

Campbell, K.J., Kinnear, S., and Thame, A. (2015). Auv technology for seabed characterization and geohazards assessment. *The Leading Edge*, 34(2), 170–178.

Chaturvedi, N., Sanyal, A.K., McClamroch, N.H., et al. (2011). Rigid-body attitude control. *Control Systems, IEEE*, 31(3), 30–51.

Felemban, E., Shaikh, F.K., Qureshi, U.M., Sheikh, A.A., and Qaisar, S.B. (2015). Underwater sensor network applications: A comprehensive survey. *International Journal of Distributed Sensor Networks*, 2015, 1–14.

Guckenheimer, J. and Holmes, P. (1983). *Nonlinear oscillations, dynamical systems, and bifurcations of vector fields*, volume 42. New York Springer Verlag.

Holmes, P., Jenkins, J., and Leonard, N.E. (1998). Dynamics of the kirchhoff equations i: Coincident centers

of gravity and buoyancy. *Physica D: Nonlinear Phenomena*, 118(3), 311–342.

Khalil, H.K. (2002). *Nonlinear systems*, volume 2. Prentice hall Upper Saddle River.

Kirchhoff, G. (1869). Ueber die bewegung eines rotationskörpers in einer flüssigkeit. *Journal für die reine und angewandte Mathematik*, 71, 237–262.

Lee, T., Leoky, M., and McClamroch, N.H. (2010). Geometric tracking control of a quadrotor uav on se (3). In *Decision and Control (CDC), 2010 49th IEEE Conference on*, 5420–5425. IEEE.

Leonard, N.E. (1997). Stability of a bottom-heavy underwater vehicle. *Automatica*, 33(3), 331–346.

Nair, S. and Leonard, N.E. (2007). Stable synchronization of rigid body networks. *Networks and Heterogeneous Media*, 2(4), 597.

Sanyal, A., Fosbury, A., Chaturvedi, N., and Bernstein, D. (2009). Inertia-free spacecraft attitude tracking with disturbance rejection and almost global stabilization. *Journal of guidance, control, and dynamics*, 32(4), 1167–1178.

Sarlette, A., Sepulchre, R., and Leonard, N.E. (2009). Autonomous rigid body attitude synchronization. *Automatica*, 45(2), 572–577.

Warier, R.R., Sinha, A., and Sukumar, S. (2014). Spacecraft attitude synchronization and formation keeping using line of sight measurements. In *World Congress*, volume 19, 8311–8316.

Weißmann, S. and Pinkall, U. (2012). Underwater rigid body dynamics. *ACM Transactions on Graphics (TOG)*, 31(4), 104.